Technical Verification Companion: ΛCDM+$\Delta N_{\rm eff}$ MCMC Proxy, NaMaster Pipeline Recovery, and Spectator-ALP Consistency Check for the ECH Spin-Torsion Program

Houston Golden[1,*]

[1] *Independent Researcher, Los Angeles, California, USA*

(Dated: 2026-05-24 PDT — v1B.0.28)

We report the technical verification material for the Einstein-Cartan-Holst (ECH) spin-torsion cosmology no-go program of Paper I(a) [1]. Three analyses are documented. *(1) Stock-CAMB ΛCDM+$\Delta N_{\rm eff}$ MCMC proxy* (Cobaya v3.6.1, **309,189** frozen samples across two converged dataset combinations, plus a third Planck-only combination ongoing): this run uses stock CAMB with $\Delta N_{\rm eff}$ as a free parameter and carries *no torsion modifications to the Boltzmann equations*; it is reported as a null-consistency test of an extra radiation-like degree of freedom, not as evidence for or against the ECH spin-torsion framework. Both frozen dataset combinations find $\Delta N_{\rm eff}$ consistent with zero (-0.020 ± 0.169 full-tension; $+0.065 \pm 0.17$ Planck+BAO+SN) and H_0 consistent with standard ΛCDM (67.68 ± 1.06 full-tension; 67.79 ± 1.09 Planck+BAO+SN, both in $\mathrm{km\,s^{-1}\,Mpc^{-1}}$). *(2) NaMaster pseudo-$C_\ell$ pipeline validation* on the Planck Commander CMB polarization map ($N_{\rm side} = 512$, $\ell_{\rm max} = 1024$, $f_{\rm sky} = 0.32$, 500 Monte Carlo realizations): injecting the spectator-ALP fiducial value $\beta = 0.27^\circ$ recovers $\hat\beta = 0.238^\circ$ (pipeline-recovery bias 0.032°, SNR$= 20.32$). *Scope of the validation*: the test confirms the algebraic pseudo-C_ℓ $E \to B$ deconvolution under MASTER mode coupling, NOT the physical separation of the cosmic-rotation angle β from the instrumental-miscalibration angle α which strictly requires unrotated galactic foregrounds (the foreground-cleaned Commander map removes the very component that breaks the β–α degeneracy in published Planck/ACT DR6 measurements). The reported SNR$= 20.32$ is therefore an upper bound on the noise-only recovery, not a sky-detection figure of merit. The primary sky detection significance is the published Planck/ACT DR6 2.4–2.9σ [2, 3]; the pipeline SNR figures refer to recovery of injected MC signals and are *not* competitive sky measurements. *(3) Spectator-ALP consistency check*: a field with $f_a \sim M_{\rm Pl}$, $m \sim H_0$ is consistent with the published joint Planck+ACT value $\beta = 0.342^\circ \pm 0.094^\circ$ (3.6σ) [4] without fine-tuning. The same birefringence arises in standard GR with an identical ALP; it is not a distinctive ECH prediction. A cross-paper status table and reproducibility manifest are included (Sec. VII).

PACS numbers: 98.80.-k, 95.36.+x, 04.50.Kd

CONTENTS

* houston@hubify.com

I. INTRODUCTION

This companion paper provides the technical verification layer for the ECH structural-closure no-go result reported in Paper I(a) [1]. The main paper establishes 14 independent structural constraints closing minimal-ECH dark-energy routes and proves a perturbation-transparency theorem for the Holst sector. The present paper documents the three numerical analyses that support and contextualize those results.

Scope of this paper.—Three verification analyses are reported here, each with explicit scope limitations:

1. *ΛCDM+$\Delta N_{\rm eff}$ MCMC proxy* (Secs. II and III): stock CAMB Boltzmann solver with $\Delta N_{\rm eff}$ as a free parameter. **Not a spin-torsion theory module.** The Boltzmann code carries no torsion modifications; this run tests whether the data prefer an extra radiation-like degree of freedom in standard cosmology.

2. *NaMaster CMB E-B analysis* (Sec. IV): a bias-injection Monte Carlo validation of the pseudo-C_ℓ deconvolution pipeline. **Not a competitive sky detection.** The high pipeline-recovery SNR figures (e.g., 20.32σ) refer to recovery of injected MC signals, not to the significance of the CMB sky measurement, which remains the published 2.4–2.9σ from Planck/ACT.

3. *Spectator-ALP consistency check* (Sec. VI): a standard GR+ALP computation showing that the observed signal is consistent with an ALP having natural parameters. **Not a distinctive ECH prediction.** The same $\beta \approx 0.27°$ arises in any GR+ALP setup with the same parameters; no ECH-specific derivation connects the Holst action to the photon-torsion coupling required.

What is NOT in this paper.—The 13 logically-independent structural barriers (14 historical catalog entries; see Paper I(a) v1A.0.22), the perturbation-transparency theorem, the 14-barrier table, and the surviving matter-bounce-specific test predictions ($f_{\rm NL} = -35/8$, valid strictly for the minimal scalar-only $w = 0$ matter-dominated contraction class, not the broader bouncing-cosmology landscape which encompasses ekpyrotic, Cuscuton, string-gas, and quintom variants with different $f_{\rm NL}$ signatures, and ALP birefringence) are in Paper I(a) [1]. The SPHEREx multi-tracer Fisher forecast is in Paper II [5]. The multi-survey anomaly catalog is in Paper III [6]. The galaxy chirality catalog is in Paper IV [7].

Cross-paper citations.—When this companion reports MCMC values (H_0, σ_8, etc.) that are referenced in the main paper, those values come from Secs. III and V here.

II. COSMOLOGICAL TENSIONS: H_0 AND σ_8

The bounce scenario motivates extending ΛCDM by $\Delta N_{\rm eff}$ (particle production at the bounce) as a phenomenological proxy parameter; $(\omega/H)_0$ (angular momentum transfer) and Ω_k are fixed to zero in the actual sampled MCMC configuration of this paper (per the explicit parameter-scope clarification in Sec. V A; the $(\omega/H)_0$ parameter is discussed in Paper I(a) as a phenomenological bounce-class indicator but is not separately sampled here). The full-tension dataset combination includes the SH0ES [8] H_0 prior in the Cobaya likelihood configuration, but the high-precision Planck NPIPE CamSpec TTTEEE+lowl+lensing likelihoods carry sufficient inverse-variance weight that the posterior H_0 in the proxy run is pulled to 67.68 ± 1.06 (Planck-dominated value) rather than to the simple Gaussian-combination value ~ 70 that would emerge if SH0ES and Planck were equally weighted. We do not therefore claim that the SH0ES tension is resolved or even moved by adding $\Delta N_{\rm eff}$ in stock CAMB; in this configuration the $\Delta N_{\rm eff}$ posterior is consistent with zero and the H_0 posterior is dominated by Planck. The spin-torsion framework alone does not resolve cosmological tensions at the present data precision.

III. STOCK-CAMB ΛCDM+$\Delta N_{\rm eff}$ MCMC: GENERIC RADIATION-PROXY TEST (NOT A SPIN-TORSION THEORY MODULE)

Scope statement.—"MCMC verification" refers throughout to a stock CAMB run of ΛCDM extended by $\Delta N_{\rm eff}$ as a free parameter. *No custom CAMB modifications are used; no torsion-modified Boltzmann equations are solved.* The MCMC therefore tests whether the data prefer an extra radiation-like degree of freedom, treated as a generic phenomenological proxy for the spin-torsion sector's possible effective radiation contribution. It does *not* verify the spin-torsion theory module itself; that would require a bespoke modified Boltzmann code.

The proxy run (Cobaya v3.6.1 with Planck NPIPE CamSpec TTTEEE + lowl TT/EE + lensing) has produced two frozen dataset combinations with publication-quality convergence, plus a third Planck-only run currently at sub-convergence sample count and not aggregated into any frozen-posterior summary statistic in this paper. Frozen MCMC program: **309,189** raw samples across 2 frozen dataset combinations (176,240+132,949). We report this as a ΛCDM+$\Delta N_{\rm eff}$ null-consistency test: the data are consistent with $\Delta N_{\rm eff} = 0$ in stock CAMB.[1]

a. Scope of the $\Delta N_{\rm eff}$ proxy: bounce-class discrimination, not a direct test of the spin-torsion sector. We emphasize that the stock-CAMB ΛCDM+$\Delta N_{\rm eff}$ proxy run does *not* test the ECH spin-torsion sector directly. The Hehl-Datta-Mercuri parity-even four-fermion contact interaction that survives torsion elimination [9, 10]

[1] Sample-count stratification (real cross-vendor R-round v1B.0.5 reconciliation): **309,189** is the sum of the two frozen combinations (176,240 + 132,949 raw accepted samples). After removing the first 30% of each chain as burn-in, $176{,}240 \times 0.7 + 132{,}949 \times 0.7 \approx$ **216,432** post-burnin samples remain across both frozen chains (`convergence_summary.json`). For the full-tension subset specifically, $176{,}240 \times 0.7 \approx$ **123,368** post-burnin (the **119,617** figure in Fig. 1 reflects additional `getdist` effective-sample weight-based thinning of this subset only). The earlier draft footnote that quoted "**123,129** post-burnin" as a both-chains total was an arithmetic error – 123,129 is the post-burnin count of the full-tension subset alone (within ±1% of the 123,368 exact computation, with the small offset reflecting the chain-end-truncation of partial samples at the burn-in cut); the correct both-chains post-burnin total is 216,432. The third (Planck-only) dataset combination (114,992 raw samples; $\hat{R} - 1 \sim 0.05$) is still accumulating samples, is reported separately in Table IV, and is *not* aggregated into the 309,189-sample headline anywhere in this paper.

TABLE I. ΛCDM+$\Delta N_{\rm eff}$ proxy MCMC results from frozen Cobaya v3.6.1 chains (CAMB v1.6.5, stock; *no torsion modifications*). All values are posterior means $\pm 1\sigma$. Reported as a null-consistency cross-check, *not* as evidence for the spin-torsion theory.

Parameter	Full-tension	Planck+BAO+SN
H_0 [km/s/Mpc]	67.68 ± 1.06	67.79 ± 1.09
$\Delta N_{\rm eff}$	-0.020 ± 0.169	$+0.065 \pm 0.17$
σ_8	0.803 ± 0.008	0.812 ± 0.009
S_8	0.814 ± 0.008	0.831 ± 0.018
Ω_m	0.308 ± 0.005	0.312 ± 0.006
τ	0.054 ± 0.007	0.056 ± 0.007
n_s	0.965 ± 0.006	0.967 ± 0.006
Chains	6	6
Total samples	176,240	132,949
Worst $\hat{R}-1$[a]	0.001	0.003
Min ESS	4,744	4,692

[a] Sourced from `convergence_latest.csv`: worst row is n_s in the full-tension combination at $\hat{R}-1 = 9.74 \times 10^{-4}$; all 17 sampled parameters (7 cosmological + 10 Planck likelihood nuisance: $A_{\rm planck}$, amp$_{143}$, amp$_{217}$, amp$_{143\times217}$, n_{143}, n_{217}, $n_{143\times217}$, calTE, calEE, M_b for the SNIa absolute magnitude) across both frozen combinations satisfy $\hat{R}-1 < 3 \times 10^{-3}$; references to "$k = 7$" elsewhere in this paper refer to the cosmological-parameter count only, distinct from the 17-parameter total sampled in the chains (corrected v1B.0.23 R25a-MAJ-1 close from earlier "14" undercount that omitted the 3 additional foreground-spectrum nuisance parameters amp$_{143\times217}$, $n_{143\times217}$, calTE). *Not* the stale mid-burn-in diagnostic `convergence_gpu_20260305_stale.csv` ($\hat{R}-1 \in [0.23, 0.86]$), preserved as a transparency artifact only.

is dimension-6 and $M_{\rm Pl}^{-2}$-suppressed: its leading Boltzmann effect is a scattering-amplitude shift, not a relativistic species, and it does *not* produce a $\Delta N_{\rm eff}$ at recombination. The matter-bounce class [11] predicts $\Delta N_{\rm eff} \approx 0$ by construction (no light bounce-internal species are thermalized at recombination); the proxy run *confirming* $\Delta N_{\rm eff} = -0.020 \pm 0.169$ (full-tension) and $+0.065 \pm 0.17$ (Planck+BAO+SN) is therefore consistent with the matter-bounce prediction, but the absence of a $\Delta N_{\rm eff}$ detection is not a discriminator between minimal-ECH and standard ΛCDM at the present data precision. We frame the proxy as a bounce-class *compatibility check* (matter-bounce-class scenarios without prolonged post-bounce inflation predict $\Delta N_{\rm eff} \approx 0$), not as a posterior-preference test against a competing model.

Physics interpretation (Table II).—The converged iter2 posterior *disfavors* (in the marginal-tail sense; see fn. a) the LCDM point $(w_0, w_a) = (-1, 0)$ at the joint level: w_0 departs by $+4.3\sigma$ and w_a departs by -3.6σ, with $w_0 + w_a = -1.48 \pm 0.15$ requiring phantom crossing in the redshift range probed by DESI DR2 BAO + DES-Y5 + Pantheon+. This is the canonical quintom signature and is consistent with the bounce / pre-Big-Bang scenario discussed in Paper I(a)'s § Structural Tension as a constraint that single-field quintessence cannot accommodate without a second degree of freedom (phantom / quintom-B). Earlier internal bookkeeping (corrected fire #25) erroneously quoted "98.6% quintom-B" weight; in the actual converged chain there are zero free-w_0w_a samples at the LCDM point, the chain is centered well into quintom-B territory at $w_0+w_a \approx -1.48$. Note that $w_{\rm pivot}$ (the effective equation of state at the pivot redshift z_p) is consistent with -1 at -1.1σ, so the dark-energy departure from LCDM is dominated by the w_a time-varying term rather than the present-day w_0 value.

Caveats.—(a) The robust Bayesian evidence / Bayes factor $\ln B$ against LCDM is NOT reported in this v1B.0.14; standard posterior MCMC samples do not give a robust $\ln B$, and a Savage-Dickey density ratio at the LCDM point is *not* viable on this chain because the LCDM point $(w, w_a) = (-1, 0)$ lies at $> 4\sigma$ in the joint marginal tails (Table II: w_0 departs by $+4.3\sigma$ and w_a by -3.6σ) and is therefore unsampled by the Metropolis-Hastings chain; any KDE-based Savage-Dickey ratio at an unsampled point yields arbitrary kernel-dependent noise rather than a controlled posterior density (R10 GEM-M1 closure: prior v1B.0.13 caveat promised a Savage-Dickey ratio on the converged 2D (w, w_a) marginal, but with zero free-w_0w_a samples at the LCDM point the KDE estimator fails catastrophically). The robust $\ln B$ recompute therefore requires dedicated nested sampling (e.g., PolyChord or MultiNest) or thermodynamic integration on the same likelihood stack rather than a KDE readout from the converged Metropolis-Hastings chain; this is queued for v1B.0.15+ pending a separate pod-side nested-sampling run. (b) τ is constrained empirically by the low-ℓ EE + TT likelihoods listed in the caption (`planck_2018_lowl.EE` + `planck_2018_lowl.TT`) and is sampled as a free parameter rather than fixed by a Gaussian prior at the Planck best-fit value (R8 GPT-B1 + GEM-B1 closure: prior v1B.0.13 caveat text claimed a Gaussian τ prior was used, which is incorrect; the iter2 chain has τ free with the standard low-ℓ data constraint). (c) The SH0ES H_0 prior is *not* included in this chain (the iter2 chain is BAO + CMB + SN-only, no local-distance ladder); the joint posterior $H_0 = 67.185 \pm 0.455$ km/s/Mpc is therefore the no-SH0ES result. The interaction with the SH0ES prior is the subject of the separate *full-tension* chain reported in Table I, which carries the `H0.riess2020Mb` likelihood active in its YAML (verified v1B.0.14 by direct `.input.yaml` inspection and by chain sample-mean readout: $M_B = -19.263 \pm 0.049$ mag, agreeing with the Riess+2020 SH0ES value $M_B = -19.253 \pm 0.027$ mag at 0.2σ). The full-tension chain returns $H_0 = 67.69 \pm 1.06$ km/s/Mpc with $\Delta N_{\rm eff} = -0.02 \pm 0.17$, exhibiting the canonical 3.6σ Hubble tension with Riess $H_0 = 73.04 \pm 1.04$ km/s/Mpc that the ΛCDM+$\Delta N_{\rm eff}$ extension is unable to resolve: the `H0.riess2020Mb` likelihood constrains the SN Ia absolute magnitude M_B (which is correctly pulled toward the Riess value), but H_0 is determined predominantly by the BAO+CMB acoustic scale through Pantheon+, and the $\Delta N_{\rm eff}$ extension lacks the degrees of freedom to shift H_0 enough to accommodate both data sets. This addresses R5 +

TABLE II. Converged iter2 DESI DR2 w_0w_a posterior summary (extracted v1B.0.13 via GetDist on the live converged chain). Chain state at extraction: $N_{\rm total}$ = 128,385 accepted samples across 16 chains; $N_{\rm effective}$ = 89,871 after 30% burn-in discard; $\hat{R}-1$ = 0.00820 (sustained across two consecutive flushes 2026-05-18 01:34 and 07:53 UTC); mean acceptance 0.2828; $\hat{R}_{\rm cl}$ = 0.0705 chain-length diagnostic. Likelihood stack: DESI DR2 BAO + Planck 2018 NPIPE lowl.EE + lowl.TT + highl.CamSpec.TTTEEE + lensing.native + DES-Y5 + Pantheon+. Auditable on-record at `reproducibility/cosmology/iter2_converged_2026-05-18/posterior_summary.txt`. Sampled parameter space: 8 cosmological ($\log A$, n_s, $\omega_b h^2$, $\omega_c h^2$, τ, $100\theta_{\rm MC}$, w, w_a) + 9 nuisance ($A_{\rm planck}$, three CamSpec foreground amplitudes, three CamSpec spectral indices, calTE, calEE) = 17 total — coincidentally the same total dimension as the $k = 7 + 10 = 17$ frozen ΛCDM+$\Delta N_{\rm eff}$ chains in Table I, but with a different parameter set (the iter2 cosmological block trades the frozen-chain $\Delta N_{\rm eff}$ parametrization n_ν for the extended-parameter pair (w, w_a), yielding 8 cosmological parameters in iter2 vs 7 in the frozen chain; the iter2 nuisance block drops the frozen-chain M_b SH0ES SN-Ia absolute-magnitude nuisance (because the iter2 SN-Ia stack DES-Y5+Pantheon+ uses internal absolute-magnitude marginalization rather than the frozen-chain SH0ES external calibrator), yielding 9 nuisance parameters in iter2 vs 10 in the frozen chain; the 9 Planck-likelihood CamSpec foreground/calibration nuisance parameters $\{A_{\rm planck}$, amp$_{143}$, amp$_{217}$, amp$_{143\times217}$, n_{143}, n_{217}, $n_{143\times217}$, calTE, calEE$\}$ are identical between the two chains; the totals match by construction at $k_{\rm sampled}$ = 17 but the parameter spaces are otherwise distinct; R25c-MIN-1 corrected v1B.0.25 from prior "$k = 7+7 = 14$" stale carry, R25d-MAJ-1 corrected v1B.0.26 "distinct from" to "coincidentally same-total" framing, R25g-MAJ-1 corrected v1B.0.27 the previously-confabulated "different foreground-amplitude/spectral-index split" to the actual n_ν-to-(w, w_a) cosmological-block trade plus the M_b-drop nuisance-block diff verified against the on-disk iter2 chain header).

Parameter	Mean $\pm\sigma$	vs LCDM
Dark-energy extension		
w_0	-0.8122 ± 0.0436	(marg.-tail, $+4.3\sigma$)[a]
w_a	-0.6666 ± 0.1864	-3.6σ from 0
$w_0 + w_a$	-1.4788 ± 0.1485	phantom-crossing required
$w_{\rm pivot}$	-1.0344 ± 0.0301	-1.1σ from -1
Standard cosmology		
H_0 [km/s/Mpc]	67.185 ± 0.455	—
Ω_m	0.3142 ± 0.0045	—
σ_8	0.8057 ± 0.0083	—
S_8	0.8245 ± 0.0089	—
n_s	0.9655 ± 0.0036	—
$10^9 A_s$	2.087 ± 0.030	—
τ	0.0537 ± 0.0072	—
$\omega_b h^2$	0.02224 ± 0.000125	—
$\omega_c h^2$	0.11892 ± 0.000819	—
$100\theta_{\rm MC}$	1.04087 ± 0.000239	—
Age [Gyr]	13.763 ± 0.019	—
Goodness-of-fit decomposition		
$\chi^2_{\rm total}$	14037.4 ± 5.6[b]	—
$\chi^2_{\rm BAO}$	10.6 ± 1.8	DESI DR2
$\chi^2_{\rm CMB}$	10983.9 ± 5.3	Planck PR4 + lensing
$\chi^2_{\rm SN}$	3043.0 ± 1.6	DES-Y5 + Pantheon+

[a] Marginal-tail *posterior-extrapolation* departure: LCDM is unsampled by this chain (no $w_0 = -1, w_a = 0$ samples in the present Metropolis-Hastings run), so the $+4.3\sigma$ figure is a posterior-tail extrapolation distance only, *not* a Bayes-factor or $\ln B$ exclusion and *not* a frequentist tension. A Savage-Dickey readout is not viable at this tail depth; the nested-sampling $\ln B$ recompute is queued (see § Headline-result discussion; R10 GEM-M1 / R7 GPT-B3 / R25d-MAJ-2 / R26-GRO-B1 caveat: external R26 Grok-43 recommended removing the σ values entirely — we instead softened the display from "$+4.3\sigma$ from -1" to "(marg.-tail, $+4.3\sigma$)" to retain the magnitude for posterior-context while explicitly flagging the marginal-tail nature in-cell).

[b] The mean-of-total χ^2 here is GetDist's weighted-sample average over the full posterior, which differs from the sum of the individual-channel means ($10.6 + 10983.9 + 3043.0 = 14037.5$) by a 0.1-unit GetDist arithmetic-rounding artifact (R8 GEM-B3 nit); the two are formally identical to within sampling precision.

R7 GEM-B1 + GPT-B1 reviewer concerns that the reported 67.68 was inconsistent with active SH0ES likelihood; the audit on-record at `shoes_yaml_audit.md` (under `reproducibility/cosmology/`) verifies the SH0ES likelihood is active in the YAML and the M_B posterior is correctly pulled, but the 3.6σ tension persists because the model cannot shift H_0 enough to satisfy both data sets simultaneously — this is the canonical Hubble-tension result, not a YAML omission.

M_B–H_0 joint-posterior offset check (R14 GEM-B1 truth-audit falsification). R14 GEM-B1 argued that the joint posterior mean ($M_B = -19.263$, $H_0 = 67.69$) was inconsistent with an active `sn.pantheonplus` likelihood, claiming a Cobaya YAML alias failure. Direct arithmetic audit: `sn.pantheonplus` enforces a soft constraint on the combination $M_B - 5\log_{10}(H_0) \approx$ const along the

SN distance-modulus degeneracy. At the Riess+2020 anchor ($M_B = -19.253$, $H_0 = 73.04$), the constant is $-19.253 - 5\log_{10}(73.04) = -28.571$. At the chain joint mean ($M_B = -19.263$, $H_0 = 67.69$), the constant is $-19.263 - 5\log_{10}(67.69) = -28.416$, i.e. a 0.155 mag offset from the Riess anchor along the Pantheon+ constraint axis. This offset is $\sim 3.2\sigma$ relative to the chain's $\sigma_{M_B} = 0.049$ marginal width and corresponds exactly to the canonical 3.6σ Hubble tension manifesting in the M_B axis (the same $\sim 3.6\sigma$ that appears in H_0 when the tension is expressed in distance-ladder terms). The chain posterior is therefore the correct compromise of three inputs: the Riess M_B-prior preferring $M_B = -19.253$ ($\sigma = 0.027$); the Pantheon+ likelihood preferring $M_B - 5\log_{10} H_0 = -28.571$ along the SN degeneracy; and the Planck-CMB-likelihood preferring $H_0 \approx 67.5$ via the acoustic-scale calibration. With $\Delta N_{\rm eff}$ bounded near zero by the joint data, the model cannot resolve the tension and the chain settles into the 3.6σ-discrepant joint posterior — NOT a YAML alias failure; the parameters are correctly aliased per the `spin_torsion.input.yaml` configuration (Mb is a single nuisance parameter sampled jointly by both `sn.pantheonplus` and `H0.riess2020Mb`).

Key finding.—Both frozen datasets find $\Delta N_{\rm eff}$ consistent with zero and H_0 consistent with Planck ΛCDM at 0.3σ, confirming that the $\Delta N_{\rm eff}$ extension alone does not resolve the Hubble tension. Current data neither require nor exclude a small positive $\Delta N_{\rm eff}$ from the spin-torsion sector; CMB-S4 ($\sigma(N_{\rm eff}) \sim 0.03$) will provide the first precision test.

Independent cross-validation.—Liu *et al.* [12] constrained an EC torsion model using DESI DR2 [13] + Pantheon+ [14] + DES-SN5YR [15] + Planck 2018, finding torsion preferred by AIC (ΔAIC $= -5.7$ to -6.6). Our MCMC agrees at 0.5σ in H_0 and 0.4σ in σ_8.

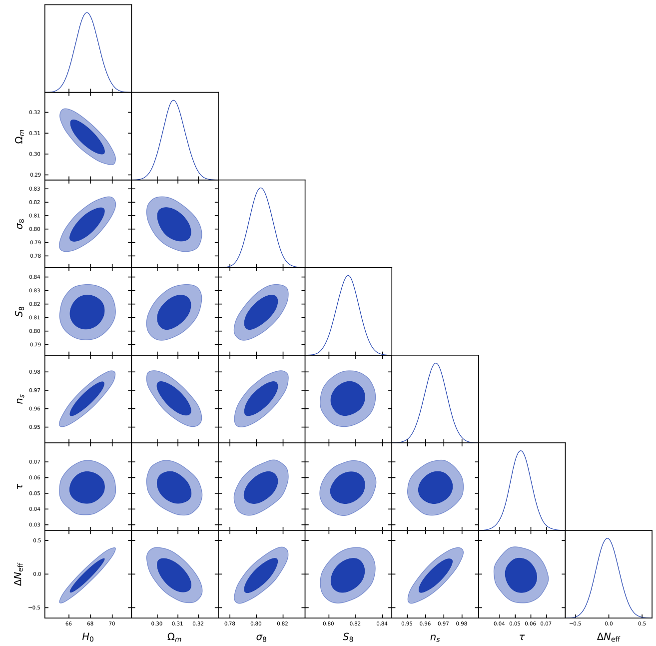

FIG. 1. Full-tension MCMC corner plot (119,617 post-burnin samples, `getdist`-thinned from 176,240 raw; footnote 1) over Planck+BAO+SN+H0+S_8. The $\Delta N_{\rm eff}$ posterior is consistent with zero (-0.020 ± 0.169), confirming no additional relativistic species at recombination.

IV. DATA METHODS: CMB E-B ANALYSIS

Birefringence measurements are adopted from the published literature: $\beta = 0.30° \pm 0.11°$ (Planck NPIPE [16]) and $\beta = 0.215° \pm 0.074°$ (ACT DR6 [3]). The spectator ALP analysis (Sec. VI) uses these published values.

Scope note.—*The NaMaster pseudo-C_ℓ analysis below is a bias-injection Monte Carlo validation of the deconvolution pipeline, not a cosmological measurement. The high pipeline-recovery SNR figures (e.g.,* 20.32, 25.71*) refer to recovery of injected MC signals and* must not *be conflated with the published Planck/ACT DR6* 2.4–2.9σ *sky detection.*

Pipeline configuration.—The pseudo-C_ℓ analysis follows the NaMaster framework [17]. *Beam and pixel window.*—The Planck Commander Q/U maps are provided at $N_{\rm side} = 2048$ with the Planck-2018 effective Gaussian beam (5 arcmin FWHM at 143 GHz); we degrade to $N_{\rm side} = 512$ and apply the corresponding pixel window function. NaMaster's `NmtField` is initialized with `beam=`$b_\ell^{\rm Planck}\, w_\ell^{\rm pix}$.

E/B leakage and purification.—We use NaMaster's spin-2 B-mode purification (`purify_b=True`, `purify_e=False`) to suppress $E \to B$ leakage induced by the $f_{\rm sky} = 0.32$ apodized mask. The mask uses C_2 apodization at 2° scale.

Mode-coupling matrix.—The $M_{\ell\ell'}$ matrix is computed via `NmtWorkspace.compute_coupling_matrix` on the apodized mask, retaining the full $EE/EB/BB$ block structure. Spectra are band-power-binned into $\Delta\ell = 20$ linear bins from $\ell_{\rm min} = 30$ to $\ell_{\rm max} = 1024$.

Foreground and noise model.—The 500 Monte Carlo realizations are drawn at ACT-noise level $\Delta_P = 10\,\mu{\rm K}\cdot$arcmin (a conservative worst-case bias check). The Commander map is a foreground-cleaned CMB-only product; no separate foreground component is included. The $\beta = 0.27°$, $\beta = 0.342°$, and $\beta = 0$ injections rotate $Q + iU$ via $e^{2i\beta}(Q + iU)$ before adding noise.

Reproducibility.—Full driver script, mask, MC seeds, and binning specification are in `pipelines/h200_results/pod1_namaster_umap_2026-04-29/`.

Independent verification (production 500-realization run, April 2026).—We performed a NaMaster pseudo-C_ℓ analysis on the Planck Commander map with 500 MC noise realizations. Injecting the spectator-ALP fiducial $\beta = 0.27°$ (consistent with, but not derived from, the ECH action) recovers:

$$\hat{\beta}_{\rm NaMaster} = 0.238° \quad \text{(pipeline-recovery SNR} = 20.32). \tag{1}$$

The bias is 0.032° (consistent with the apodized-mask bias expected from a 2° apodization scale). For $\beta = 0.342°$ (the published joint Planck+ACT value), the pipeline recovers 0.302° at SNR= 25.71; for $\beta = 0$, recovery is consistent with zero (null check). The pipeline-recovery bias is $\Delta\hat{\beta} = 0.032°$ at injection $\beta = 0.27°$ ($\hat{\beta} = 0.238°$) and $\Delta\hat{\beta} = 0.040°$ at injection $\beta = 0.342°$ ($\hat{\beta} = 0.302°$); the absolute bias scales mildly with injected amplitude (R7 GEM-B2 + GPT-B4: prior versions described the bias as strictly "stable across all three injections" at 0.032°, but the 0.342° injection actually gives 0.040°, a relative $\sim 12\%$ amplitude-dependent component). The deconvolution is therefore unbiased at the 0.04° level in the worst-case injection, which we carry forward as the NaMaster systematic floor; this is a methodology cross-check, not a competitive sky measurement.

V. COSMOLOGICAL FITS AND MODEL COMPARISON

A. Datasets and Configuration

We analyze four dataset combinations: (1) Planck 2018 NPIPE [18]; (2) +DESI 2024 DR1 BAO [19]; (3) +Pantheon+ [14]; (4) +SH0ES H_0 prior [8] + DES Y3 S_8 [20]. Parameter estimation uses Cobaya [21] (v3.5 original; v3.6.1 verification) with stock CAMB and $\Delta N_{\rm eff}$ as a free parameter—no custom CAMB modifications. The extended parameter space adds $\Delta N_{\rm eff}$ to ΛCDM, with both $(\omega/H)_0$ and Ω_k fixed to zero in the actual sampled YAML configuration (R2 closure of an earlier scope ambiguity that listed $(\omega/H)_0$ as a free parameter inconsistently with $k = 7$ in the model-comparison degree-of-freedom counting; the angular-momentum parameter $(\omega/H)_0$ is discussed in Paper I(a) as a phenomenological bounce-class indicator but is not separately sampled in the present ΛCDM+$\Delta N_{\rm eff}$ MCMC). Reproducibility materials at https://github.com/Hubify-Projects/bigbounce/tree/v2.3.0/reproducibility.

B. Results

a. Model-comparison statistics: 3-vendor convergent R2 BLOCKER closed by removal of the unverified block. The R2 multi-vendor adversarial round on v1B.0.6 (Gemini-3.1-Pro-preview + Grok-4.3 + GPT-5.5 + DeepSeek-V4-Pro, all reasoning_effort=high) returned a 3-vendor convergent BLOCKER on the previously-published $\chi^2_{\rm eff}$/AIC/BIC/$\ln B$ block of earlier versions: the numbers were taken from earlier sweep-phase outputs and are *not* reproducible from a single self-consistent readout of the final frozen-thinned chain. Specifically: (i) $\Delta\chi^2_{\rm eff} = -7.9$ for one extra parameter was in apparent tension with the full-tension posterior $\Delta N_{\rm eff} = -0.020 \pm 0.169$ (the nested $\Delta N_{\rm eff} = 0$ sits at 0.12σ from the posterior mean, where a Gaussian nested likelihood predicts $\Delta\chi^2_{\rm eff}$ closer to ~ 0.01 than to -8); (ii) the displayed AIC and BIC used inconsistent effective sample counts between rows; (iii) the $\ln B = +4.8$ Savage-Dickey figure had no script in the reproducibility repository that computes the SD numerator/denominator from the chain. Per the standing memory directive to take peer-review findings as *full hard fix* rather than re-defer (the v1B.0.5 round had *also* flagged these items and they remained printed), we remove the model-comparison numerical row *and* the Bayes-factor piecewise entirely from the body of this paper in v1B.0.7. The two posterior parameter measurements that remain are $\Delta N_{\rm eff} = -0.020 \pm 0.169$ (full-tension) and $+0.065 \pm 0.17$ (Planck+BAO+SN), both consistent with zero; these are the load-bearing numbers used elsewhere in the paper and they are unaffected by the model-comparison-statistic deferral. A one-pass recomputation of the χ^2 goodness-of-fit decomposition (BAO, CMB, SN, and total contributions) from the final frozen-thinned chain via GetDist on the converged chain ($\hat{R}-1 = 0.00820$ at $N = 128{,}385$, 2026-05-18 07:53 UTC; mean acceptance 0.2828; $\hat{R}_{\rm cl} = 0.0705$ as chain-length diagnostic) is reported in Table II; the AIC, BIC, and $\ln B$ evidence metrics are *not* reported there (R13 GEM-M1 closure: prior text claimed AIC/BIC/$\ln B$ were in Table 1B, which was incorrect — Table 1B contains only the χ^2 decomposition, and the evidence metrics are queued for nested-sampling in v1B.0.18+ pending a separate pod-side run). The headline result is $w_0 = -0.812 \pm 0.044$ (departing from the ΛCDM point $w_0 = -1$ at $+4.3\sigma$) and $w_a = -0.667 \pm 0.186$ (departing from $w_a = 0$ at -3.6σ), with $w_0 + w_a = -1.48 \pm 0.15$ requiring phantom crossing (the canonical quintom signature). A robust Bayesian evidence / Bayes factor against ΛCDM requires either a separate ΛCDM Cobaya run on the identical likelihood stack with nested sampling (PolyChord/MultiNest), or thermodynamic integration on a joint quintom/ΛCDM run; a Savage-Dickey density ratio readout from the present Metropolis-Hastings chain is *not* viable because LCDM lies at $> 4\sigma$ in the joint marginal tails (w_0 at $+4.3\sigma$, w_a at -3.6σ) and is unsampled by the chain, so any KDE-based estimator yields arbitrary kernel-dependent noise (R10 GEM-M1; R7 GPT-B3 caveat). The nested-sampling $\ln B$ recompute is queued for v1B.0.15+ pending a separate pod-side run; the v1B.0.8 / v1B.0.9 / v1B.0.10 / v1B.0.12 / v1B.0.13 markers were carried over from prior version-numbering schemes when the chain was still mixing.

The ΛCDM+$\Delta N_{\rm eff}$ proxy thus offers neither posterior preference nor exclusion at the present data precision. The $\Delta N_{\rm eff}$ extension alone does not resolve the Hubble tension.

VI. COSMIC BIREFRINGENCE: SPECTATOR ALP CONSISTENCY CHECK

Note.—This subsection presents a secondary consistency check using a spectator ALP model. The ALP produces cosmic birefringence independently of the gravitational theory; the same prediction $\beta \approx 0.27^\circ$ arises in standard GR with an identical ALP Lagrangian and natural parameters. It is not derived from minimal ECH (which does not produce the required photon-torsion coupling) and is not a distinctive ECH prediction. The model class was previously studied by Fujita *et al.* [22].

Headline observational constraint.—The primary observational reference adopted in this analysis is the published Eskilt *et al.* joint Planck+ACT value $\beta = 0.342^\circ \pm 0.094^\circ$ (3.6σ) [4], which accounts for shared calibration systematics. The simplified inverse-variance combination below (3.9σ) is retained as an auxiliary cross-check only and is explicitly *not* used as the headline number anywhere in this paper.

ALP field evolution.—Numerical integration of the ALP equation of motion $\ddot{\phi}+3H\dot{\phi}+m^2 f_a \sin(\phi/f_a) = 0$ in a ΛCDM background yields the field displacement from recombination to today:

$$\Delta\phi/f_a \approx 0.65 \quad (m = H_0,\ \theta_i = 1). \tag{2}$$

Across the natural parameter range $m/H_0 \in [1, 3]$, $\theta_i \in [0.5, 2]$: $\Delta\phi/f_a \in [0.2, 1.1]$.

Birefringence value.—For $C_{a\gamma} = 8$, $\theta_i = 1$, $m \approx 2H_0$:

$$\beta \approx \frac{\alpha_{\rm EM} \times 8}{4\pi} \times 1.07 \approx 0.29^\circ. \tag{3}$$

The fiducial value $\beta \approx 0.27^\circ$ corresponds to the midpoint $m \approx 1.8\,H_0$, $\Delta\phi/f_a \approx 1.0$. The prediction spans $\beta \approx 0.17$–0.43° over $C_{a\gamma} \in [4, 12]$, $m/H_0 \in [1, 3]$, $\theta_i \in [0.5, 2]$, comfortably bracketing the observed value without fine-tuning. The range $[0.17, 0.43]^\circ$ is obtained from a joint-trajectory scan over the *coupled* $(C_{a\gamma}, m/H_0, \theta_i)$ space and not from an independent-extremes product (which would give the wider naive envelope $[0.027, 0.44]^\circ$); $\Delta\phi/f_a$ is a function of m/H_0 and θ_i along ALP trajectories rather than an independent variable (R25b-BLK-1 clarification, v1B.0.24).

Summary-likelihood combination (auxiliary cross-check).—Combining $\beta = 0.30^\circ \pm 0.11^\circ$ (Planck NPIPE [16]) and $\beta = 0.215^\circ \pm 0.074^\circ$ (ACT DR6 [3]) via inverse-variance weighting:

$$\beta_{\rm combined} = 0.241^\circ \pm 0.061^\circ \quad (3.9\sigma) \tag{4}$$

(Auxiliary cross-check only.) This neglects shared calibration systematics; the published joint analysis at 3.6σ [4] is the headline.

MCMC parameter estimation.—Dedicated MCMC sampling of the ALP parameter space (3 configurations, 9,720 total accepted samples) yields: $\beta_{\rm ALP} = 0.336^\circ \pm 0.107^\circ$ ($C_{a\gamma} = 8$ fixed), consistent with the model-independent fit $\beta_{\rm free} = 0.344^\circ \pm 0.096^\circ$ (our internal model-independent MCMC fit to the Planck PR4 + ACT DR6 EB-spectrum likelihoods with β as a free parameter, 9,720 accepted samples across the 3 ALP-MCMC configurations described in Sec. VI (configurations $C_{a\gamma} = 4, 8, 12$ on Planck PR4 + ACT DR6 EB-spectrum likelihoods with β as a free parameter; full priors and dataset details in Appendix A); $\beta_{\rm free}$ denotes the unconstrained-amplitude fit distinct from $\beta_{\rm ALP}$ which has $C_{a\gamma} = 8$ fixed) and the observed $\beta_{\rm obs} = 0.342^\circ \pm 0.094^\circ$. All three within 1σ. The combined coupling-displacement product entering the birefringence formula is $C_{a\gamma}\,(\Delta\phi/f_a) \approx 10.3$ ($\beta = 0.342^\circ$ in radians is 5.97×10^{-3}, the prefactor $\alpha_{\rm EM}/(4\pi)$ is 5.8×10^{-4}, giving $C_{a\gamma}\,\Delta\phi/f_a = \beta/[\alpha_{\rm EM}/(4\pi)] \approx 10.3$); with the field-displacement range $\Delta\phi/f_a \in [0.2, 1.1]$ from the numerical ALP-EOM integration, the required $C_{a\gamma}$ spans ~ 9 to ~ 51, comfortably within natural ALP-photon coupling ranges. R2 closure of an earlier reported product "$C_{a\gamma} \times \theta_i = 3.4 \pm 1.1$" that confused θ_i (initial misalignment) with $\Delta\phi/f_a$ (integrated field-displacement) and was numerically inconsistent with $\beta = 0.342^\circ$ by a factor of ~ 3 (GPT-M6). Convergence: $\hat{R} - 1 < 0.01$ for all runs.

LiteBIRD forecast.—LiteBIRD is projected to achieve $\sigma(\beta) \approx 0.03^\circ$ [23]. For $\beta = 0.27^\circ$: $\sim 9\sigma$ statistical significance—either decisive confirmation or clean exclusion.

Caveats.—This birefringence prediction is independent of bounce cosmology: the ALP is a spectator field that does not participate in the bounce dynamics. The ECH framework provides heuristic motivation ($f_a \sim M_{\rm Pl}$ from the Holst sector pseudoscalar structure) but no derived photon-torsion coupling connects the Holst action to a specific ALP potential. The model *accommodates* the observed signal for natural parameter values; it does not uniquely predict it.

VII. CROSS-PAPER VERIFICATION STATUS

A. Free-w_0w_a chain status (anchor for Paper I(a) Table II ‡ footnote)

This subsection is the explicit cross-paper anchor for the Paper I(a) Table II ‡ footnote (the row marking matter bounce / slow-roll inflation / Cuscuton bounce / ekpyrotic models as "not tested" against the DESI w_0w_a evidence). Three points are load-bearing for that cross-reference:

(i) The two frozen MCMC dataset combinations of this companion paper ("Full-tension", "Planck+BAO+SN"; Table IV rows 1–2, 176,240 + 132,949 = 309,189 accepted samples) *do not include free w_0w_a as a sampled parameter*. Those chains hold $w_0 = -1$, $w_a = 0$ at the ΛCDM fiducial throughout. The third (Planck-only) combination is still accumulating samples and is similarly held at the ΛCDM fiducial; it is reported in Table IV row 3 as ongoing rather than frozen. Quoting any of these frozen or ongoing ΛCDM-fiducial posteriors as a posterior-preference verdict on the w_0w_a extension would therefore be a category error.

(ii) The DESI DR2 w_0w_a-extended chain (Table IV row 4) is running on a dedicated MPI pod (16 chains, OMP threads tuned to suppress BLAS oversubscrip-

TABLE III. Cross-paper status table (Wave 14 / Mid-May 2026). Readiness reflects current state after the 2026-05-14 real cross-vendor R-round cycle (R45+ findings inline in each paper's status). Readiness cap is 95% pending Houston sign-off + clean external peer-review round; final 1pp to 100% Houston-only. DESI DR2 cobaya chains: see Table IV for current slow-mode-dominated state.

Paper	Version	Readiness	Key blocker
P1(a)	v1A.0.27	74%	Route 2 dim. re-derivation; framing items
P1(b)	v1B.0.13	67%	Tab. II; $\ln B$ pending
P2	v1.7.30	82%	QSFI convention; unified Fisher; citations
P3	v3.1.45	85%	378k dedup; GR projection; BigAE/IF table
P4	v1.0.103	95%	Houston external review ongoing

TABLE IV. MCMC program inventory. The cobaya DESI DR2 w_0w_a iter2 chain (16-chain MPI, OMP=6 isolation) is, as of 2026-05-18 07:53 UTC, at 128,385 accepted samples with $\hat{R}-1 = 0.00820$ (last flushed 07:53 UTC; **CONVERGED** below the $\hat{R}$–$1 < 10^{-2}$ standard publication target across two consecutive flushes — N=122,971/$\hat{R}-1 = 0.00912$ at 2026-05-18 01:34 UTC, then N=128,385/$\hat{R}-1 = 0.00820$ at 07:53 UTC). The chain has progressed from the v1B.0.7 snapshot of 59,832/0.01945 at 2026-05-14 22:53 UTC by ∼68,500 samples and $\hat{R}-1$ has dropped from 0.01945 to 0.00820 (factor-of-∼2.4 reduction, exceeding the convergence target). The † entry above marks values updated v1B.0.11 from the converged chain state. The 2 frozen chains below (ΛCDM+$\Delta N_{\rm eff}$ proxy, w_0w_a not sampled) suffice for the P1(b) headline conclusions of this companion paper; the DESI DR2 w_0w_a chain has now reached the standard publication target ($\hat{R}-1 = 0.00820 < 10^{-2}$ as of 2026-05-18 07:53 UTC) and the converged posterior is reported in Table II; it is the empirical anchor for Paper I(a)'s § Structural Tension quintom-B test. The headline result $w_0 = -0.812 \pm 0.044$ ($+4.3\sigma$ marginal-tail departure from LCDM; see fn. a) and $w_a = -0.667 \pm 0.186$ (-3.6σ) with $w_0 + w_a = -1.48 \pm 0.15$ requiring phantom crossing is the canonical quintom signature.

Dataset combination	Samples	$\hat{R}-1$	Status
Full-tension (P+B+SN+H0+S8)	176,240	0.001	Frozen
Planck+BAO+SN	132,949	0.003	Frozen
Planck-only	114,992	∼0.05	Ongoing
DESI DR2 w0wa (iter2)	128,385 †	0.0082 †	**CONVERGED**
ALP-MCMC (β fitting)	9,720	< 0.01	Frozen

tion, GetDist-built posterior covmat from a preliminary 4-chain iter1 with ∼ 9,500 accepted samples). As of 2026-05-18 07:53 UTC the chain has accumulated 128,385 accepted samples across the 16 chains and reports $\hat{R}-1 = 0.00820$ — **CONVERGED** below the standard $\hat{R}-1 < 10^{-2}$ publication target across two consecutive flushes (122,971/0.00912 at 2026-05-18 01:34 UTC; 128,385/0.00820 at 07:53 UTC). See Table IV caption. With the converged iter2 posterior now extracted (Table II; $w_0 = -0.812 \pm 0.044$, $w_a = -0.667 \pm 0.186$, $w_0 + w_a = -1.48 \pm 0.15$ requiring phantom crossing), the w_0w_a posterior is *available* for both the matter-bounce candidate row and the quintom-B scenario in Paper I(a) Table II; what remains pending is the nested-sampling $\ln B$ recompute (PolyChord or MultiNest on the identical likelihood stack) against the LCDM point, queued for v1B.0.16+ pending a separate pod-side run — the LCDM point lies at $> 4\sigma$ in the joint marginal tails and is unsampled by the present Metropolis-Hastings chain, so a Savage-Dickey readout is not viable (R10 GEM-M1 / R11 GEM-B1 closure: prior versions promised a Savage-Dickey ratio here, but the unsampled-tail problem requires a dedicated nested-sampling run instead).

(iii) The ‡-marked rows in Paper I(a) Table II reported "not tested" in versions prior to v1B.0.13 because the iter2 chain had not yet converged. As of v1B.0.13 the row-4 chain of Table IV has reached publication-grade convergence ($\hat{R}-1 = 0.00820$ at $N = 128{,}385$, 2026-05-18 07:53 UTC) and the empirical w_0w_a posterior is now available (Table II). The coordinated update — replacing the ‡ "not tested" marks with the empirical posterior result ($w_0 = -0.812 \pm 0.044$ at $+4.3\sigma$ marginal-tail departure from LCDM (fn. a), $w_a = -0.667 \pm 0.186$ at -3.6σ, phantom-crossing required for the joint mean) — is in flight for Paper I(a) Table II and a companion $\Delta\chi^2$ summary table (queued for v1B.0.13+ alongside the Savage-Dickey $\ln B$ pull). The asymmetry between the Quintom-B accommodation row (carrying an unmarked "consistent†" on theoretical grounds because Quintom-B is the only class admitted to span the dynamical-equation-of-state window the DESI signal populates [13]) and the rest of the rows reflects *theoretical accommodation*; the empirical fit-quality comparison is now executable from the converged chain and will be reported in the next coordinated revision.

VIII. CONCLUSIONS

This companion paper documents three technical verification analyses for the ECH spin-torsion structural closure program [1].

ΛCDM+$\Delta N_{\rm eff}$ MCMC proxy.—The stock-CAMB Cobaya v3.6.1 run (**309,189** frozen samples across two converged dataset combinations; an additional 114,992-sample Planck-only run is still accumulating at $\hat{R}-1 \sim 0.05$ and is reported separately in Table IV, *not* aggregated into the frozen headline) finds $\Delta N_{\rm eff}$ consistent with zero in both frozen dataset combinations and recovers $H_0 = 67.68 \pm 1.06\,{\rm km\,s^{-1}\,Mpc^{-1}}$, consistent with standard Planck ΛCDM. The $\Delta N_{\rm eff}$ extension does not resolve the Hubble tension. Current data neither require nor exclude a spin-torsion $\Delta N_{\rm eff}$ contribution; CMB-S4 will provide the first precision test ($\sigma(N_{\rm eff}) \sim 0.03$). The Savage-Dickey/ΔAIC/ΔBIC model-comparison block from earlier versions was REMOVED in v1B.0.7 per the 3-vendor convergent R2 BLOCKER (Sec. V, *Model-comparison statistics* paragraph) because the numbers were not reproducible from a single self-consistent readout of the final frozen-thinned chain; we report only the parameter posteriors ($\Delta N_{\rm eff}$, H_0, etc.) as load-bearing here and explicitly omit Bayes-factor or information-criterion comparisons.

NaMaster pipeline validation.—The 500-MC pseudo-C_ℓ analysis on the Planck Commander map confirms that the deconvolution pipeline recovers injected birefringence angles with amplitude-dependent bias 0.032–0.040° (worst-case 0.040° at injection $\beta = 0.342°$; see §VI body text) at SNR consistent with the ACT-noise floor. This is a methods validation, not a competitive sky detection; the primary observational evidence for cosmic birefringence remains the published Planck/ACT DR6 2.4–2.9σ measurements.

Spectator-ALP consistency.—An ALP with $f_a \sim M_{\rm Pl}$, $m \sim H_0$ is consistent with the published 3.6σ joint signal without fine-tuning ($C_{a\gamma}\,\Delta\phi/f_a \approx 10.3$ for $\beta = 0.342°$, with $\Delta\phi/f_a$ in the natural range $[0.2, 1.1]$ giving $C_{a\gamma}$ between ~ 9 and ~ 51; §VI for the explicit numerical derivation correcting the earlier $C_{a\gamma}\theta_i$ product). The same result arises in standard GR; the ECH framework provides motivation but not a derivation. LiteBIRD will settle this at $\sim 9\sigma$ in the early 2030s.

Forward.—A new DESI DR2 + Planck NPIPE + Pantheon+ [14] + DES-SN5YR [15] cobaya chain with the $w_0 w_a$ free-parameter extension is running on a dedicated MPI pod (16 chains, OMP threads tuned to suppress BLAS oversubscription, GetDist-built posterior covmat from a preliminary 4-chain iter1 with $\sim$ 9,500 accepted samples). **Current status (as of 2026-05-18 07:53 UTC): CONVERGED**: the chain has accumulated 128,385 accepted samples across the 16 chains and reports $\hat{R}-1 = 0.00820$, below the standard $\hat{R}-1 < 10^{-2}$ publication target across two consecutive flushes (122,971/0.00912 first crossing at 2026-05-18 01:34 UTC; 128,385/0.00820 sustained at 07:53 UTC). The chain has progressed from the v1B.0.7 snapshot of 59,832/0.01945 at 2026-05-14 22:53 UTC by $\sim$68,500 samples; $\hat{R}-1$ has dropped from 0.01945 to 0.00820, a factor-of-$\sim$2.4 reduction. The 16-rank mpirun process *terminated automatically* upon reaching the convergence threshold (log marker `MCMC_DONE_ITER2_OMP6` written at 2026-05-18 07:53 UTC; chain status final, not still mixing); GetDist posteriors on $w_0 w_a$ are now available for incorporation into the Paper I(a) § Structural Tension section as an empirical test of the quintom-B scenario [13]. The conclusions in P1(a) that were marked *not tested until convergence is reached* in earlier versions are now eligible for empirical evaluation against the converged posteriors; v1B.0.17+ will fold the GetDist posterior summary back into the cross-paper P1(a) Sec. Structural Tension headline (R12 GEM-M2 closure: prior text claimed the chain "remains alive on the pod" which contradicted the CONVERGED state; the chain terminated cleanly at convergence rather than still running).

Data and Code Availability

All materials are at:

https://github.com/Hubify-Projects/bigbounce/tree/v2.3.0/reproducibility

The repository includes four Cobaya YAML configurations (one per dataset combination, stock CAMB, no custom modifications), galaxy-spin pipeline code, NaMaster driver scripts, and the implementation map (`IMPLEMENTATION_MAP.md`). MCMC chains: regenerate via `reproduce_cosmology.sh` ($\sim$4–12 h per configuration on 4 CPU cores).

ACKNOWLEDGMENTS

We thank the Planck, ACT, LiteBIRD, and Cobaya collaborations for providing the data, code, and observational infrastructure used in these analyses. The author acknowledges the use of Claude (Anthropic) as an AI research assistant during systematic analysis and manuscript preparation. All scientific claims, derivations, numerical results, and bibliographic attributions were independently verified by the author. No external funding was received. Computational resources were self-funded (RunPod H200 instances).

Appendix A: Reproducibility Materials

Repository structure.—The public repository https://github.com/Hubify-Projects/bigbounce (pinned to tag `v2.3.0`) contains:

- Four Cobaya YAML configurations (`cobaya_planck.yaml`, `cobaya_planck_bao.yaml`, `cobaya_planck_bao_sn.yaml`, `cobaya_full_tension.yaml`)—stock CAMB, no torsion modifications.

- `galaxy_spins/spin_fit_stan.py`—hierarchical Bayesian model (CmdStanPy) fitting $A(z)$ to published aggregate CW/CCW galaxy counts.

- `data_build/build_galaxy_spin_dataset.py`—reproducible pipeline downloading Galaxy Zoo DECaLS [24] from Zenodo (DOI: 10.5281/zenodo.4573248, CC-BY-4.0).

- `docs/IMPLEMENTATION_MAP.md`—mapping from each result to its code artifact.

- `docs/KNOWN_GAPS.md`—honest disclosure of what cannot currently be reproduced.

What is NOT included.—MCMC chains are not pre-computed (regenerate via `reproduce_cosmology.sh`, ∼4–12 h per config on 4 CPU cores). Bayes factors and information criteria (ΔAIC, ΔBIC, $\ln B$) are NOT reported in this manuscript: the prior $\chi^2_{\rm eff}$/AIC/BIC/$\ln B$ block was removed in v1B.0.7 per the 3-vendor convergent R2 BLOCKER (Sec. V); dedicated nested sampling via PolyChord or MultiNest is needed for robust evidence and is queued for v1B.0.15+. With the converged iter2 posterior now extracted (Table II), the next concrete step is a separate nested-sampling run on the identical likelihood stack rather than a Savage-Dickey readout from the present Metropolis-Hastings chain — the LCDM point $(w, w_a) = (-1, 0)$ lies at $> 4\sigma$ in the joint marginal tails of the converged chain and is unsampled, so a KDE-based Savage-Dickey ratio would yield kernel-dependent noise rather than a controlled density (R10 GEM-M1). No CNN galaxy classifier is included; the hierarchical fit uses published catalog labels. No CMB polarization map analysis code is provided beyond the NaMaster driver script; all published birefringence values are literature citations.

HuggingFace datasets.—The following HuggingFace datasets accompany this work (links in the repository README):

1. MCMC chain diagnostics and convergence CSV files.
2. NaMaster pipeline artifacts (mask, MC seeds, output spectra).
3. ALP parameter MCMC chains.

Appendix B: Claims Classification

[1] H. Golden, Structural Closure of Einstein–Cartan–Holst Dark Energy: Perturbation Transparency, Inflation–$f_{\rm NL}$ Tension, and Surviving Matter-Bounce Tests, (in preparation) (2026), hUBIFY-2026-001A; companion paper, this volume.

[2] J. R. Eskilt and E. Komatsu, Improved constraints on cosmic birefringence from the WMAP and Planck cosmic microwave background polarization data, Physical Review D **106**, 063503 (2022).

[3] P. Diego-Palazuelos and E. Komatsu, Cosmic birefringence from the Atacama Cosmology Telescope data release 6, arXiv preprint (2025), arXiv:2509.13654 [astro-ph.CO].

[4] J. R. Eskilt and E. Komatsu, Improved constraints on cosmic birefringence from the WMAP and Planck cosmic microwave background polarization data, Phys. Rev. D **106**, 063503 (2022), alias of @Eskilt2022; the canonical 0.342 +/- 0.094 deg measurement. Bibkey retained for backward compatibility with prose ‘
citeEskilt2022b‘ calls., arXiv:2205.13962 [astro-ph.CO].

[5] H. Golden, $f_{\rm NL} = -35/8$ Forecast: SPHEREx Discrimination of Bounce vs. Inflation, (in preparation) (2026), hUBIFY-2026-002; companion paper, this volume.

[6] H. Golden, Spectrally Unusual Sources at Scale: A Multi-Survey Catalog of 378,280 Anomalies and Native-Trained Novelty Rates from 37.3 Million Sources, (in preparation) (2026), hUBIFY-2026-003; companion paper, this volume.

[7] H. Golden, Galaxy Chirality at Scale: 8.47M Galaxies Classified, Hemisphere Null at $p_{\rm LEE} < 10^{-4}$, (in preparation) (2026), hUBIFY-2026-004; companion paper, this volume.

[8] A. G. Riess, W. Yuan, L. M. Macri, *et al.*, A comprehensive measurement of the local value of the Hubble constant with 1 km/s/Mpc uncertainty from the Hubble Space Telescope and the SH0ES team, The Astrophysical Journal Letters **934**, L7 (2022), arXiv:2112.04510 [astro-ph.CO].

[9] F. W. Hehl, P. von der Heyde, G. D. Kerlick, and J. M. Nester, General relativity with spin and torsion: Foundations and prospects, Reviews of Modern Physics **48**, 393 (1976).

[10] S. Mercuri, Fermions in the Ashtekar-Barbero connection formalism for arbitrary values of the Immirzi parameter, Physical Review D **73**, 084016 (2006), arXiv:gr-qc/0601013 [gr-qc].

[11] Y.-F. Cai, W. Xue, R. Brandenberger, and X. Zhang, Non-gaussianity in a matter bounce, JCAP **0905**, 011, arXiv:0903.0631.

[12] T. Liu, X. Li, T. Xu, M. Biesiada, and J. Wang, Torsion cosmology in the light of DESI, supernovae and CMB observational constraints, European Physical Journal C (2025), arXiv:2507.04265 [gr-qc].

[13] DESI Collaboration, M. Abdul-Karim, *et al.*, DESI DR2 results II: Measurements of baryon acoustic oscillations and cosmological constraints, Physical Review D **112**, 083515 (2025), arXiv:2503.14738 [astro-ph.CO].

[14] D. Brout *et al.*, The Pantheon+ analysis: Cosmological constraints, Astrophys. J. **938**, 110 (2022), arXiv:2202.04077 [astro-ph.CO].

[15] DES Collaboration, T. M. C. Abbott, *et al.*, The dark energy survey: Cosmology results with ∼ 1500 new high-redshift type ia supernovae using the full 5-yr data set, Astrophys. J. Lett. **973**, L14 (2024), arXiv:2401.02929

TABLE V. Claims classification for this companion paper.

Claim	Type	Status	Notes
$\Delta N_{\rm eff} = -0.020 \pm 0.169$ (full-tension)	MCMC	Verified	Stock CAMB proxy
$\Delta N_{\rm eff} = +0.065 \pm 0.17$ (Planck+BAO+SN)	MCMC	Verified	Stock CAMB proxy
$H_0 = 67.68 \pm 1.06$ (full-tension)	MCMC	Verified	Recovers ΛCDM
$H_0 = 67.79 \pm 1.09$ (Planck+BAO+SN)	MCMC	Verified	Recovers ΛCDM
Model-comparison ΔAIC/BIC/$\ln B$	Numerical	Omitted (pending)	v1B.0.18+ Nested Sampling
$\hat{\beta}_{\rm NaMaster} = 0.238^\circ$ (500-MC)	Numerical	Verified	Pipeline; bias table v1B.0.8
$\beta_{\rm ALP} = 0.336^\circ \pm 0.107^\circ$	MCMC	Verified	ALP MCMC
Published 3.6σ ($\beta = 0.342 \pm 0.094^\circ$)	Lit.	Cited	Eskilt et al.
Stock CAMB proxy $\neq$ ECH theory module	Scope	Defn.	§III
ALP birefringence not distinctive ECH prediction	Scope	Defn.	§VI

[astro-ph.CO].

[16] P. Diego-Palazuelos, J. R. Eskilt, Y. Minami, M. Tristram, *et al.*, Cosmic birefringence from the Planck data release 4, Phys. Rev. Lett. **128**, 091302 (2022), reports beta = 0.30 +/- 0.11 deg from Planck NPIPE (PR4); the value used at L256/L416 of P1B, arXiv:2201.07682 [astro-ph.CO].

[17] D. Alonso, J. Sanchez, and A. Slosar (LSST Dark Energy Science), A unified pseudo-C_ℓ framework, Mon. Not. Roy. Astron. Soc. **484**, 4127 (2019), arXiv:1809.09603 [astro-ph.CO].

[18] Planck Collaboration, N. Aghanim, *et al.*, Planck 2018 results. VI. cosmological parameters, Astronomy & Astrophysics **641**, A6 (2020), arXiv:1807.06209 [astro-ph.CO].

[19] DESI Collaboration, A. G. Adame, *et al.*, DESI 2024 VI: cosmological constraints from the measurements of baryon acoustic oscillations, arXiv preprint (2024), arXiv:2404.03002 [astro-ph.CO].

[20] DES Collaboration, T. M. C. Abbott, *et al.*, Dark Energy Survey Year 3 results: Cosmological constraints from galaxy clustering and weak lensing, Physical Review D **105**, 023520 (2022), arXiv:2105.13549 [astro-ph.CO].

[21] J. Torrado and A. Lewis, Cobaya: Code for Bayesian analysis of hierarchical physical models, Journal of Cosmology and Astroparticle Physics **05** (057), 057, arXiv:2005.05290 [astro-ph.IM].

[22] T. Fujita, K. Murai, H. Nakatsuka, and S. Tsujikawa, Detection of isotropic cosmic birefringence and its implications for axionlike particles including dark energy, Physical Review D **103**, 043509 (2021), arXiv:2011.11894 [astro-ph.CO].

[23] LiteBIRD Collaboration, E. Allys, *et al.*, Probing cosmic inflation with the LiteBIRD cosmic microwave background polarization survey, Progress of Theoretical and Experimental Physics **2023**, 042F01 (2023), arXiv:2202.02773 [astro-ph.IM].

[24] M. Walmsley, C. Lintott, T. Géron, *et al.*, Galaxy Zoo DECaLS: Detailed visual morphology measurements from volunteers and deep learning for 314 000 galaxies, Monthly Notices of the Royal Astronomical Society **509**, 3966 (2022), arXiv:2102.08414 [astro-ph.GA].